Study a Structural Behavior of Eccentrically Loaded GFRP Reinforced Columns Made of Geopolymer Concrete

Hussein Talab Nhabih [a*], Ahmed M. Hussein [b], Marwa Marza Salman [a]

[a] *Department of Ceramic and Building Material, Faculty of Materials Engineering, Babylon University, Babylon, Iraq.*

[b] *Babylon Technical Institute, Al-Furat Al-Awsat Technical University, Babylon, Iraq.*

Abstract

This study investigated a modern composite material, which is a short geopolymer concrete column (GPCC) reinforced by GFRP bars. The structural performances of GPCC subjected to eccentric load were studied and compared to the normal strength concrete column (NSCC) reinforced by steel bars. In this study, the primary experimental parameters were the reinforcement bars types, load eccentricity, and concrete types. Seven short columns were tested: three normal strength concrete columns reinforced by steel bars, three geopolymer concrete columns reinforced by GFRP bars and one normal strength concrete column without reinforcement. The model dimensions chosen in the present study was a square section of 130×130 mm and a total height of 850 mm. It was shown that the steel bars contribute about 16.47% of column capacity under concentric load. Comparing with the normal strength concrete column, a geopolymer concrete column reinforced by GFRP bars showed a little increase in ultimate load (5.17%) under concentric load. Under the load eccentricity of 130 mm, a geopolymer concrete column reinforced by GFRP bars showed a significant increase in the ultimate load (69.37%). Under large eccentricity, a geopolymer concrete column reinforced by GFRP bars has an outstanding effect on the columns' ultimate load capacity. Also, the sine form can be utilized for GPCC to find the lateral deflection along with the column high at different load values up to the failure.

Keywords: Geopolymer Concrete; GFRP; Eccentric Load; Short Columns.

1. Introduction

The columns are more significant members of the structure as their weakness may cause a failure of adjacent structural elements leads to the collapse of the whole structure. There are different ways to improve column performance such as increasing the durability of the column, preventing the steel corrosion used as columns' reinforcement, etc. [1]. In this regard, Glass Fiber Polymer (GFRP) bars and the Geopolymer concrete (GPC) can be employed.

In addition of its corrosion resistant, GFRP as lightweight bars have high tensile strength, big durability, and electromagnetic impartiality [2, 3]. Geopolymer concrete (GPC), also called inorganic polymer concrete (IPC), is environmentally nonhazardous material which utilizes a geopolymer binder instead of Portland cement (PC). The manufacture of (PC) contributes nearly 6.8% of total carbon dioxide quantity [4]. This nearly adds (1600000) milliard kilo gram of (CO_2) into the environment [5]. Accordingly, this denotes more satisfying to investigate the substitute binding by less of emission of CO_2 for a concrete product. With this regard, Geopolymer binder can be utilized. The

reaction of industrial cinders produces the Geopolymer binder in silica (SiO_2) and alumina (Al_2O_3), like metakaolin, fly ash, and ground granulated blast-furnace slag with an alkaline fluid, usually a blend of sodium silicate and the solution of sodium hydroxide [6-8]. The components of Geopolymer concrete are fine and coarse aggregates, fly ash, blast-furnace slag, sodium silicate, sodium hydroxide solution, water and/or super plasticizer. Geopolymer concrete is essentially chemical and fire-resistant, low drying shrinkage, little creep, good thermal stability, excellent resistance of acid and sulphate and the best bond with reinforcing steel [9-12]. Additionally, the geopolymer concrete compressive strength is either superior or nearer than that of the normal strength concrete of similar quality [13, 14].

Several researches investigated the shear performance and flexural performance of steel reinforced geopolymer concrete [15, 16], FRP reinforced concrete [17-19] and FRP reinforced geopolymer concrete [20]. Comparatively, a small number of researches are existing that studied the performance of columns consisted of these systems [21, 22]. Generally, the ACI 440.1R-08 [23] ignores the compression associating of GFRP bars while the CSA S806-12 [24] does not recommend utilizing of GFRP bars in columns, due to their low compression strength. Depending on prior studies, the compressive strength for GFRP bars is about 30% to 70% of their tensile strength [25]. FIB Bulletin 40 [26] referred that the association of the steel bars in compression is more than the GFRP bars to carry the ultimate load of the concrete column. Based on fifteen $45 \times 25 \times 120$ cm^3 column specimens, Alsayed et al. [27] noticed that replacing the GFRP rebars with an equivalent quantity of steel rebars increased the column capacity by 12%. Based on Tobbi et al. [28], at a column's maximum load, the GFRP rebars compressive strength is 36% of their capability in tension. Also, the GFRP rebars' associating was 11% of column capability, which is convergent from that of steel rebars (13%). Additionally, they assure the GFRP rebars employing in columns if sufficient confinement is done. Sarker [29] studied the performance of columns casted by geopolymer concrete and reinforced by steel rebars. He advised that the design provisions of ordinary concrete columns might be utilized for geopolymer concrete columns with use of the suitable stress–strain relation. Sreenath et al. [30] studied the suitability of using GFRP bars to reinforce concentrically or eccentrically loaded columns. They concluded that GFRP bars are not suitable for reinforcing columns subject to concentric or eccentric loads by a small eccentricity. This conclusion was due to the practical results obtained from their practical program, which confirms that the yield load, failure load and energy absorption capacity of the reinforced columns with GFRP bars are much lower than the reinforced columns with steel bars. Sumajouw et al. [31] analyzed the reinforced geopolymer concrete columns' behaviour which is subjected to uniaxial bending and concentric load. They suggested the analytical method existed in the codes can be utilized to analyses the reinforced geopolymer concrete columns. Mohamed et al. [32] used the finite element method to analyze the reinforced columns with GFRP bars casted by geopolymer concrete or ordinary concrete utilizing the ABAQUS program. The reinforced column subjected to concentric and eccentric loads. The results obtained from the ABAQUS program were compared with the practical results, and a very large convergence between them was found. Minhao et al. [33] investigated the structural behavior of eleven air-cured reinforced columns with GFRP bars and made of geopolymer concrete subjected to concentric loads. The results showed that the ultimate load of concrete columns reinforced with GFRP bars is about 10.8% higher than the ultimate load of concrete columns reinforced with steel bars.

The present paper studied the structural performance of the Geopolymer concrete columns reinforced by GFRP bars subjected to eccentric load. Results are compared with columns made of ordinary concrete reinforced by steel bars. The properties of geopolymer concrete, normal strength concrete, GFRP bar and steel bar were studied. Additionally, the effects of the longitudinal bar types, the load eccentricity and the concrete types (normal strength concrete and Geopolymer concrete) were investigated on the load- lateral deflection curves, first cracking loads, ultimate load, failure modes, crack patterns and concrete strain variation of specimens.

2. Materials and Methods

2.1. Materials' Properties

2.1.1. Normal Strength Concrete and Geopolymer Concrete

Mix proportions (ACI 211.1-91) [34] was used to design the normal strength concrete (NSC) base on the ACI approch. The Geopolymer concrete was made of coarse and fine aggregate, Geopolymer binder, plasticizer and water. Table 1 shows the characteristics of the blast-furnace slag and fly ash oxides. The alkaline solution produced from dissolved solid sodium hydroxide into the solution of sodium silicate is used in the formation of the Geopolymer binder. The ratio of the solution of sodium silicate / solid sodium hydroxide is equal to 1.6. Based on the previous studies, thirteen groups of geopolymer binder were tested so as to find the best composition of the mixture. With this regard, durability and mechanical properties were examined [35, 36]. The natural sand was utilized as fine aggregate, and the gravel (coarse aggregate) was crushed with a maximum aggregate size (MAS) of 12.5 mm. Table 2 and Figure 1 show distributions of the particle size. Table 3 shows the mix proportions of geopolymer concrete and normal strength concrete. ASTM C469-02 [37] and ASTM C39/C39M-05 [38] were utilized to test the static-elastic modulus (E_c) and compressive strength of cylinder concrete (f_c') respectively. Each result of static-elastic modulus and compressive strength were obtained by the average of two cylinders (150×300 mm) specimens at 28 days. The average

static-elastic modulus and compressive strength of the normal strength concrete and the geopolymer concrete were 24.5 GPa, 27.3 MPa, and 32.9 GPa, 36.2 MPa, respectively.

Table 1. Characteristics of blast furnace slag and fly ash oxides (wt %)

Composition	BFS	Fly ash
SiO_2	31.30	50.13
CaO	38.11	3.08
Fe_2O_3	0.41	5.32
Al_2O_3	14.57	30.03
MgO	9.89	1.14
K_2O	0.34	2.33
SO_3	3.05	1.43
BaO	0.31	0.04
Na_2O	0.37	0.65
others	1.27	2.53
L O I	0.38	3.32

Table 2. The Particle size distribution of sand and gravel

Size of sieve (mm)	Passing (%)	
	Sand	Gravel
14	-	100
10	-	71.8
4.75	94.7	8.3
2.36	80.4	-
1.18	75.3	-
0.6	61.8	-
0.3	32.4	-
0.15	6.6	-
0.075	1.01	-
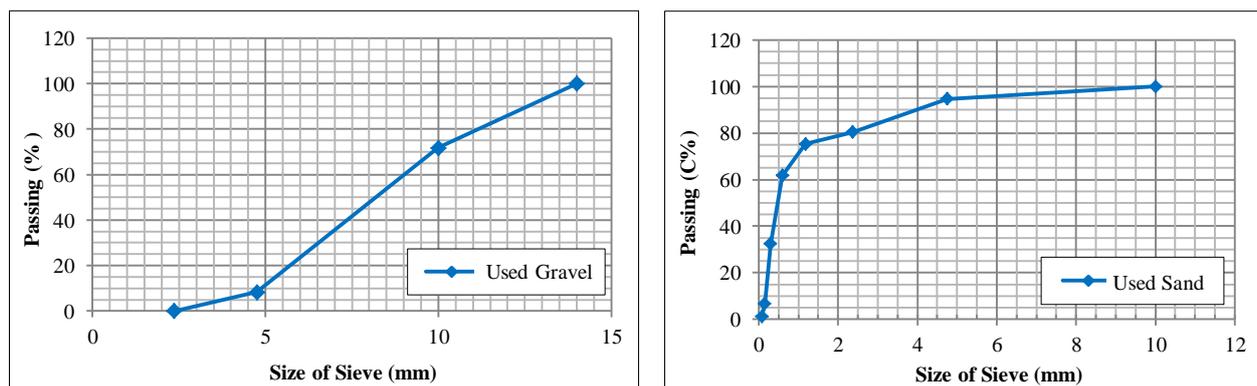
Figure 1. Grading curves of used materials

Table 3. The mix proportions of the normal strength concrete and the Geopolymer concrete (kg/m³)

Concrete type	Cement	GP binder	Water	Plasticizer	Fine aggregate	Coarse aggregate
NSC	310	-	200	-	840	950
GPC	-	450	136	5.4	610	1247

Figure 2. Static-elastic modulus test for geopolymer concrete tested at 28 days

2.1.2. Steel Reinforcement

In this study, two types of steel reinforcing rebars were utilized: first, deformed steel rebars of nominal diameter Ø4 mm as transverse ties and second, deformed steel rebar of nominal diameter Ø12 mm as longitudinal and corbel reinforcement (Ukrainian production). Based on ASTM A496-02 [39] requirements, tensile testing was performed on three samples, provided from each kind of steel reinforcing rebars. The machine was able to draw the load-displacement curve using a computer program up to the failure of the sample. Table 4 shows the test results.

Table 4. Test results of steel and GFRP reinforcing rebars

Property	Tensile strength (MPa)	Yield strength (MPa)	Compression strength (MPa)	Tensile modulus of elasticity (GPa)	Compression modulus of elasticity (GPa)
Ø4 mm steel bar	590	408	-	198	-
Ø12 mm steel bar	610	497	-	205	-
Ø12 mm GFRP bar	715	-	383	40.5	39.7

2.1.3. GFRP Reinforcement

In GFRP column samples, the longitudinal reinforcement is four high-modulus (HM) GFRP bars by diameter (12 mm), as shown in Figure 3. The GFRP bar was produced using glass fibers saturated by a vinyl ester resin. Over and above, sand coated its surface. So, the force transfer and the bond between Geopolymer concrete and bars were improved. Measuring the tensile strength according to ASTM D7205M [40], three tensile samples were tested. Up until now, due to the fiber micro-buckling, there is no standard technique for measuring the compressive properties of GFRP bars. In this regard, three 12 mm GFRP bars, by a free height twice the diameter of bars, were cut as even as enabled and were exposed to compression loads.

Figure 3. Sand coated GFRP bars

In the compression test, the GFRP bars failed by crushing while there were no buckling. Table 4 represents the results of tensile and compressive tests. Based on the compression test, average of the GFRP bars' compressive strength was 383 MPa, which was 53.6% of the tensile strength of the bars. This percent ratio of strength was lower than that stated by De Luca et al. [41] (55%) for GFRP bars but was like to that determined by Deitz et al. [42] (52%). In compression and tension, the study assumed a linear elastic behavior up to the failure of GFRP bars. Moreover, the GFRP bar's modulus of elasticity in tension and compression were like. Prior studies mentioned these assumptions.

2.2. Details of Test Samples

In this study, the primary experimental parameters are longitudinal bar types, load eccentricity and concrete types. Two kinds of longitudinal reinforcement GFRP bar and steel bar were chosen. Three eccentricities of 130 mm, 30 mm and 0 mm were selected. And, two kinds of normal strength concrete and geopolymer concrete were studied. The test sample design details are shown in Figure 4 and Table 5, where "ST" stands for the ordinary steel bar and "GF" refers to the GFRP bar.

The test samples were classified into two types. The first type labeled "NSCC" was consisted of four ordinary reinforced concrete columns, except the sample NSCC-0 denotes plain concrete without reinforcement, and served as control samples. "GPCC" consisted of three geopolymer concrete columns. For each type, three samples were tested under an eccentricity of 0, 30, and 130 mm, respectively. All seven short columns were tested: three normal strength concrete columns reinforced by steel bars, three geopolymer concrete columns reinforced by GFRP bars and one normal strength concrete column without reinforcement. All columns are identical in size and the nominal dimensions. The model dimensions chosen in the present study was a square section of 130×130 mm and a total height of 850 mm. The height between corbels is of 450 mm and every corbel head had a length of 200 mm. All samples reinforced by longitudinal bars located by symmetrical form. The transverse reinforcement was prepared by rectangular ties Ø 4 mm @ 90 mm C/C. The depth of concrete cover was 150 mm. Additional transverse and longitudinal reinforcement was prepared in corbel heads to avoid early failures in corbel heads. The reinforcement details and sample layout are shown in Figure 5.
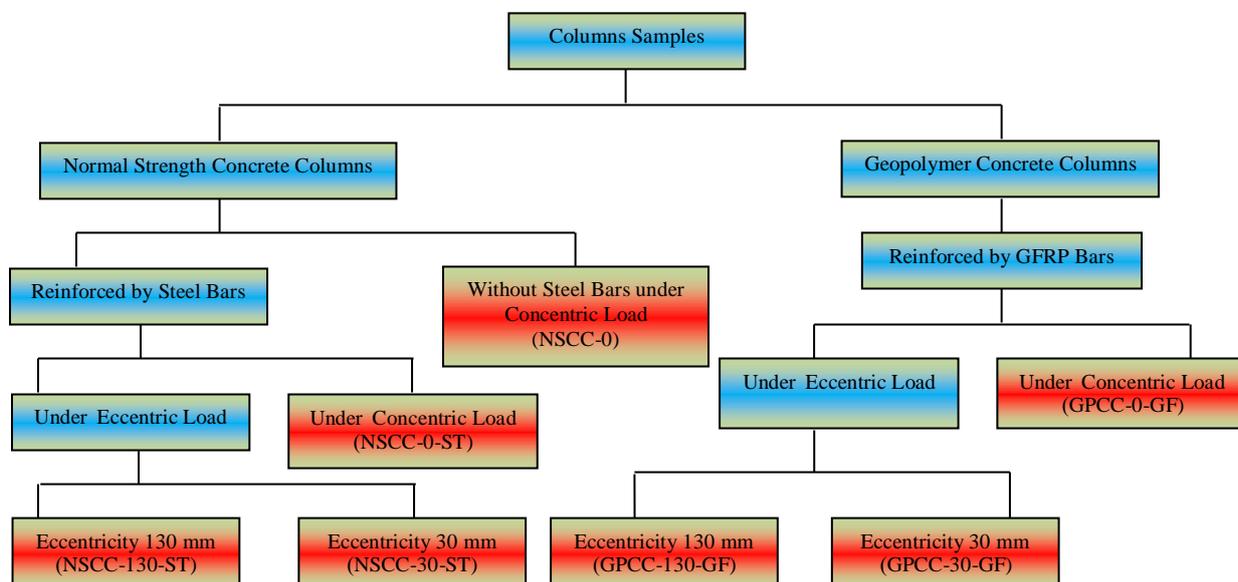
Figure 4. Schematic representation of columns samples

2.3. Casting and Curing Procedure

To prevent concrete from sticking to the mould, the inner faces of wooden column moulds were oiled. After that, the reinforcement was located in the correct location for each one of column moulds. The samples were cast in a mould made from wood with one batch. For geopolymer concrete, gravel and sand were initially mixed for 2.5 minute. Then, the geopolymer binder was mixed at the same time with gravel and sand for 3.5 minute followed to a slow adding of plasticizer and water. All moulds filled by concrete in a single layer with compaction. After one day, the samples were levered from their moulds and then all samples were immersed in a water container for 28 days. Then, white coloring used to coat the columns in order to make sure an obvious look of the crack development, and after that kept in the laboratory up to testing.
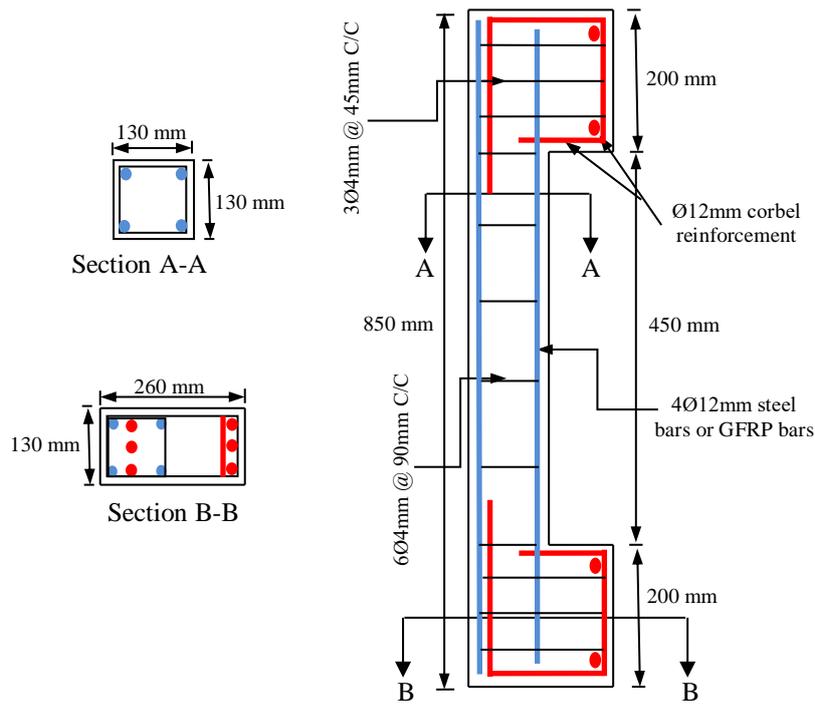
Figure 5. Reinforcement details and sample layout

Table 5. Details of the tested column samples

Samples	Longitudinal reinforcement	Longitudinal reinforcement ratio ρ %	Eccentricity (mm)
NSCC-0	0	0	0
NSCC-0-ST	ST 4Ø12	2.67	0
NSCC-30-ST	ST 4Ø12	2.67	30
NSCC-130-ST	ST 4Ø12	2.67	130
GPCC-0-GF	GF 4Ø12	2.67	0
GPCC-30-GF	GF 4Ø12	2.67	30
GPCC-130-GF	GF 4Ø12	2.67	130

2.4. Loading Condition and Test Setup

The column samples were tested in a testing machine, which has a (670 kN) capability by a hydraulic jack and a digital gauge. Two end supports made as hinged links by defined eccentricity. All columns were loaded up to failure. The force applied in stages by a loading increase speed of about 5 kN. The major properties of their structural manners were tested at each stage of loading through the test of the column samples. The result of test, which were registered through the tests, were: the first cracking load besides the ultimate load at failure, concrete strain and lateral deflections. In every load stage, notes of crack growth on the concrete column indicated by a deep felt pen. Measurements of the lateral deflection were registered at the tension side of the column in midpoint height and at a distance of 200 mm below and above midpoint height using three LVDT. The concrete strain was measured by an extensometer (strain gage) having a precision (0.002 mm). Five couples of demec discs were utilized at the midpoint of column height to measure the concrete strain. The arrangements of LVDT, demec discs and extensometer are shown in Figure 6.
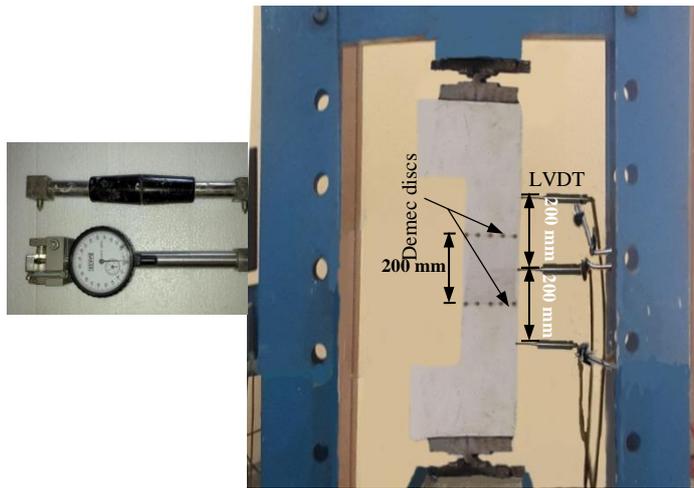
Figure 6. Arrangement of LVDT, demec discs and extensometer

3. Experimental Results

3.1. Load-lateral Deflection Curves

Lateral deflection measurements at midpoint height were registered up to the ultimate load. Recorded loads and lateral deflection at the midpoint height of columns GPCC-30-GF, NSCC-30-ST, GPCC-130-GF, NSCC-130-ST are presented in Figure 7. Testing the other columns NSCC-0, GPCC-0-GF, NSCC-0-ST under concentric loading, lateral deflection of these columns is equal to zero.
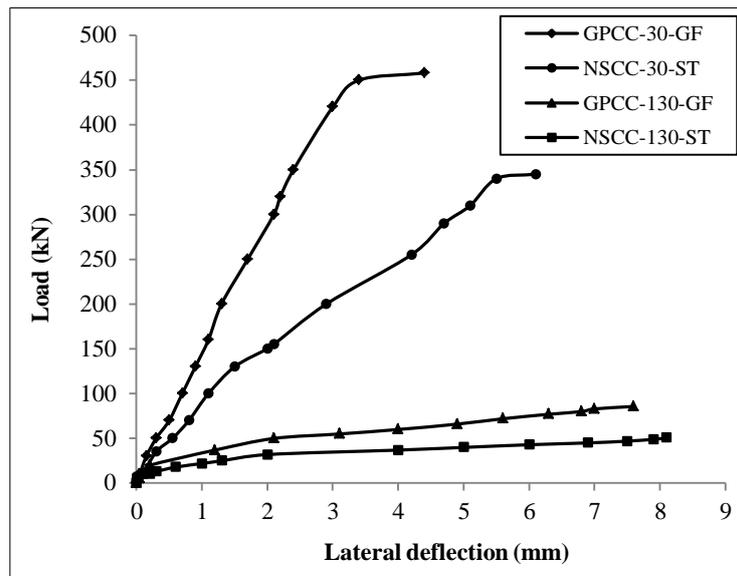
Figure 7. Load-lateral deflection at the midpoint height of tested columns

From Figure 7, the load versus lateral deflection curve has three distinctive stages. The first stage is a direct segment representing the linear elastic step. The second is a non-linear portion with a notable change of slope showing an increase of deflections (elastic-plastic stage). Finally, the third is a non-linear portion but has a minor increase in the load with a higher deflection (representing the plastic stage). Due to the higher compressive strength of GPCC, the GPCC stiffness reinforced by GFRP bars is more than the NSCC stiffness reinforced by steel bars. For the column subjected to loads along with its height, two other LVDTs were located at the lower and upper quartiles about the midpoint of height to investigate the lateral deflections increment (Figure 6). Figure 8 shows lateral deflections tested along with the height for NSCC and GPCC during different levels of the applied loads. For each one of the samples, the lateral deflections are remarkably near for one with others at lower and upper quartiles. For normal strength concrete columns, the lateral deflection at an identified location along with the height of the column, δ, is calculated applying the sine form, $\delta = \Delta. \sin(\pi x/H)$, where Δ defines the maximum lateral deflection at the midpoint of sample height, x denotes the vertical distance from the base of the sample and H is the sample height. Figure 8 shows the results calculated by the abovementioned equations and experimental results. Results exhibit an extremely high closeness for experimental with analytical results. This states that sine form of normal strength concrete columns can

utilize to geopolymer concrete columns reinforced by GFRP bars to calculate the lateral deflection along with the height of column during different loading stages up to failure. This is consistent with the study of Sarker [29].

3.2. First Cracking Load and Ultimate Load

Table 6 shows the test results for the load corresponding to the first cracking and the ultimate load. From table 6, one can see the load corresponding to the first cracking changed from (9.88%) to (60.64%) of ultimate loads. This significant variation in the proportions was due to the compressive strength, eccentricity of the load and type of longitudinal reinforcement. The columns with a concentric load or small eccentricity were under the compressive stress, and therefore, the cracks required a big load to initiate. Nevertheless, the initial cracks of the columns with high eccentricity needed a small load to initiate. Based on the experimental results in Table 6, for the NSCC-0-ST sample, the steel bars contributed 16.47% of column capacity under an axial load. This is consistent with the study of Tobbi et al. [28]. Moreover, the GPC column reinforced by the GFRP bar (GPCC-0-GF) showed a little increase (5.17%) in the ultimate load under an axial load. Whereas, it showed a distinct increase (69.37%) under the load eccentricity of 130 mm. It can note that using the geopolymer concrete column reinforced by the GFRP bar has a significant effect on the ultimate load capacity with high eccentricity. All samples of small eccentricity showed a higher ultimate load due to their different failure modes. Both of the compressive and tensile longitudinal reinforcement bars and the concrete participated in the load-bearing of the sample with small eccentricity. But for the sample with high eccentricity, just the tensile longitudinal reinforcement bars, and concrete took part and the column collapsed in tension dominated failure.
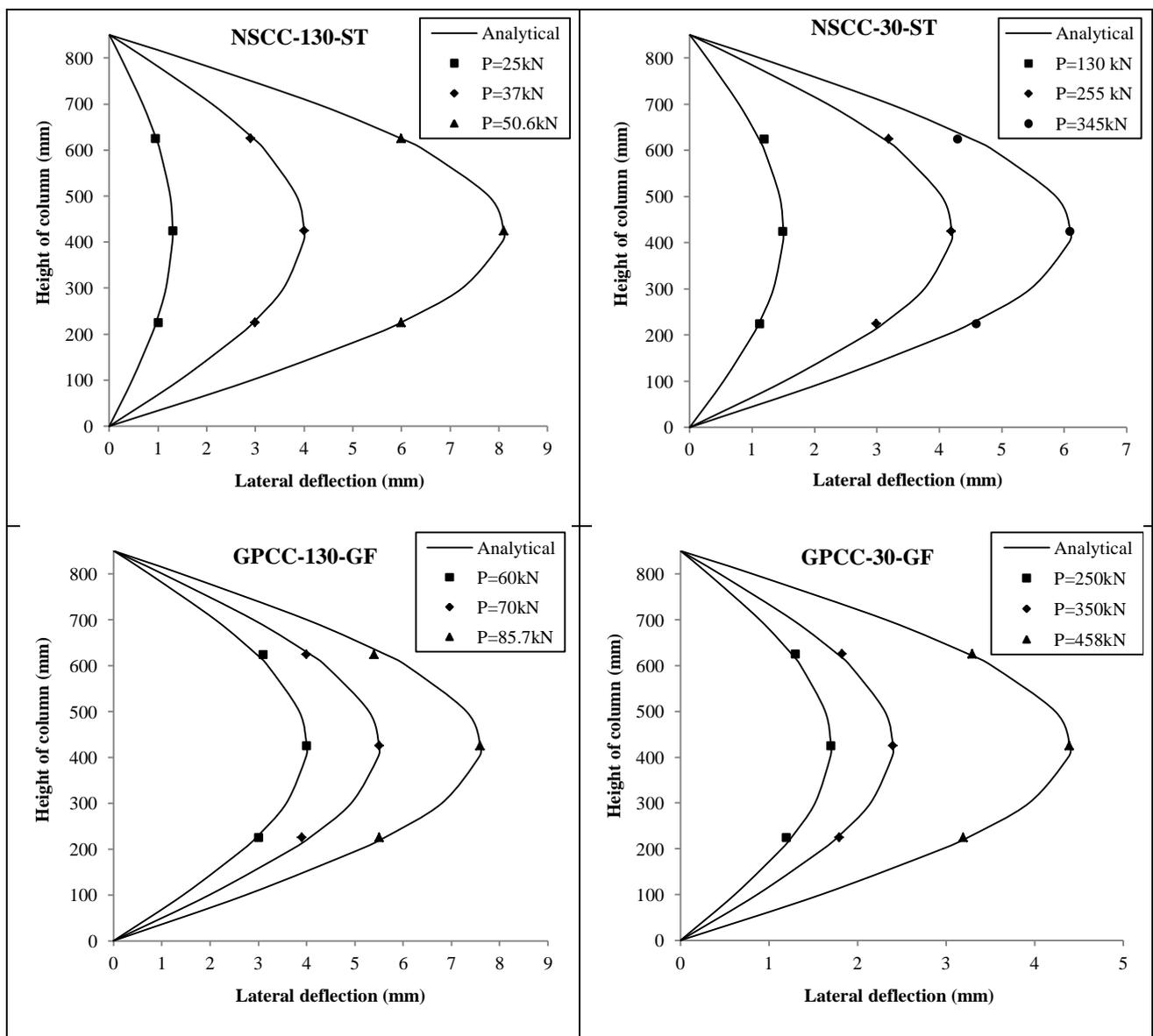
Figure 8. Analytical and the experimental lateral deflection of the tested columns

Table 6. Test results of the ultimate load and the first cracking load

Samples	Ultimate load Pu (kN)	First crack load Pcr (kN)	(Pcr/Pu) %
NSCC-0	498	302	60.64
NSCC-0-ST	580	196	33.79
NSCC-30-ST	345	130	37.68
NSCC-130-ST	50.6	5	9.88
GPCC-0-GF	610	290	47.54
GPCC-30-GF	458	250	54.59
GPCC-130-GF	85.7	20	23.34

3.3. Failure Modes and Cracks Pattern

For the column sample NSCC-0, failure occurred suddenly after reaching the ultimate load. Moreover, the columns' sample NSCC-0-ST and NSCC-30-ST collapsed in a brittle manner because of concrete cleavage and simultaneous buckling of the longitudinal reinforcement bars. Also, GPCC-0-GF and GPCC-30-GF samples failure happened suddenly in a brittle manner because of concrete crushing and simultaneous rupturing of the longitudinal reinforcement bars. This is not consistent with the study of Sreenath et al. [30]. The failure of all the above samples can be described as a compressive failure mode. Whereas the failure behavior of the remaining samples (NSCC-130-ST and GPCC-130-GF) was gradually directed toward the tension region, even the remaining outermost concrete crumbled. Consequently, NSCC-130-ST and GPCC-130-GF can be classified as a tension failure mode. The columns with concentric load or small eccentricity were under compressive stress and; therefore, the cracks needed a higher load to initiate. Because of stress concentration near the corbels, the cracks appeared firstly in this region. Under high eccentricity of loading, as the concrete tensile stress reached the ultimate tensile strength, the first cracks appeared in the middle of the column or near it through the tension face. Figure 9 shows a failure and the cracks pattern of all samples.

3.4. Strain of Concrete

Five couples of demec discs were used at the midpoint of the column height to measure the concrete strain at the chosen values of loading. Demec discs calibrated by a supplementary particular ruler. Figure 10 shows the variation of concrete strain at the midpoint height of the columns with a load increasing. When comparing the strain of concrete at the failure load of the geopolymer concrete column under axial load with the normal strength concrete column, it is noted that the strain of the geopolymer concrete column is less by about 50% of the strain of normal strength concrete column because the elastic modulus and the compressive strength of the geopolymer concrete is greater than the normal strength concrete. Also, it was observed that the concrete strain of the column NSCC-0 is almost the same as the column NSCC-0-ST, this indicates that the reinforcement bars have no significant impact on the strain of concrete in the columns under axial loads.

In the initial loading stages of the columns samples NSCC-30-ST, GPCC-30-GF, NSCC-130-ST and GPCC-130-GF, the strain of concrete on the tension side was little due to the concrete and reinforcement work together to resist the tensile deformation. Whereas in the final loading stages, the geopolymer concrete strain on the tension side was much greater than the strain of normal strength concrete due to the modulus of elasticity of the steel bars of the normal strength concrete columns much greater than the GFRP bars of geopolymer concrete columns. As for the strain on the compression side of the geopolymer concrete columns, it was almost the same in the normal strength concrete columns, despite the difference in the load value this is due to the good mechanical properties of the geopolymer concrete. Based on Figure 10, there is a pure compression zone for the samples with an axial load such as NSCC-0, NSCC-0-ST, and GPCC-0-GF or with small eccentricities such as NSCC-30-ST and GPCC-30-GF. By eccentricity increment, the compression zone decreased gradually while the tension zone appeared and developed. With this regard, the neutral axis shifted in direction of the compression zone. For all the samples, the changes of concrete strains at the midpoint height were wavy linearly or close to linear. For columns having tension and compression zones, it became more uniform.

Figure 9. Cracks pattern of failure
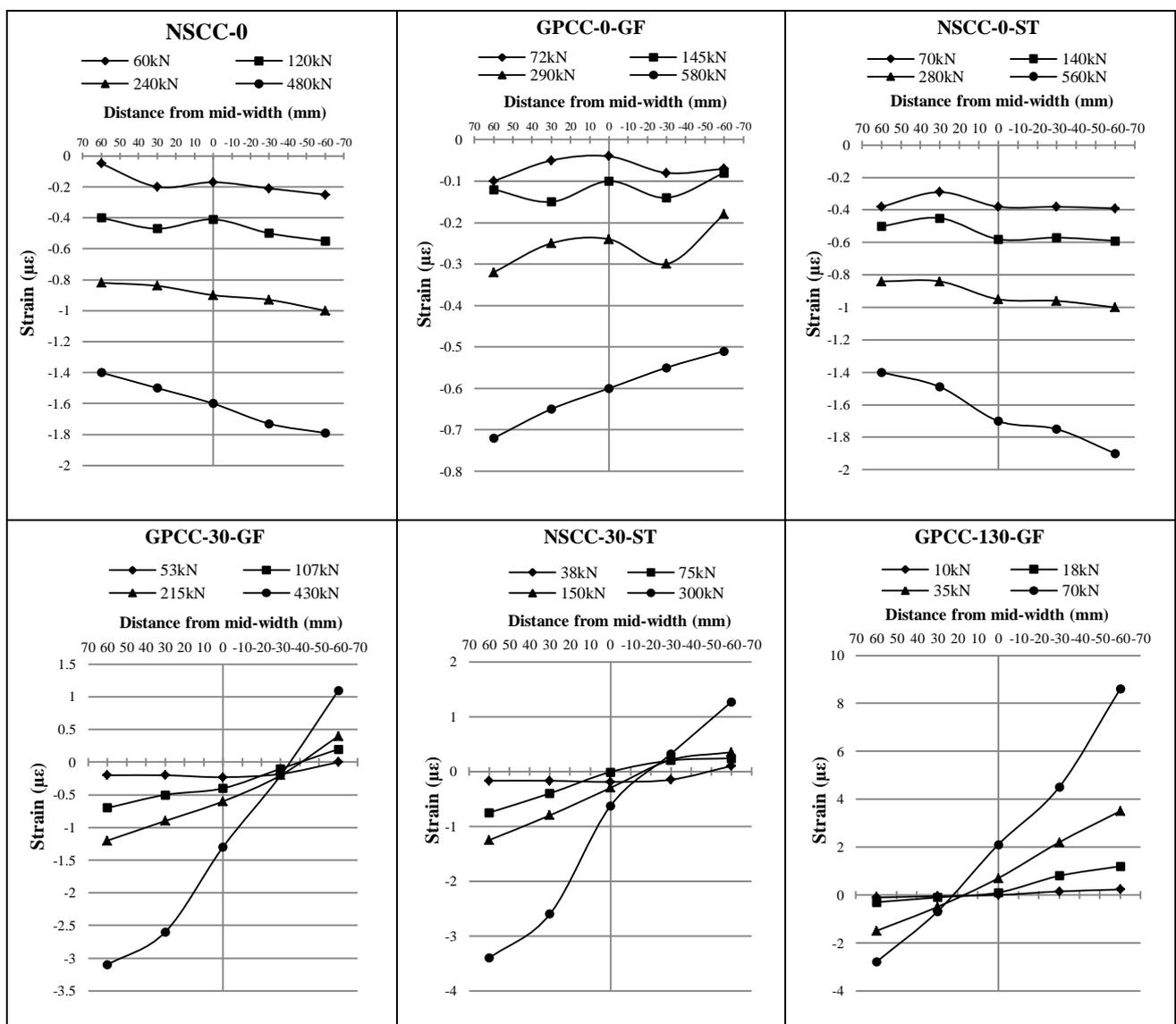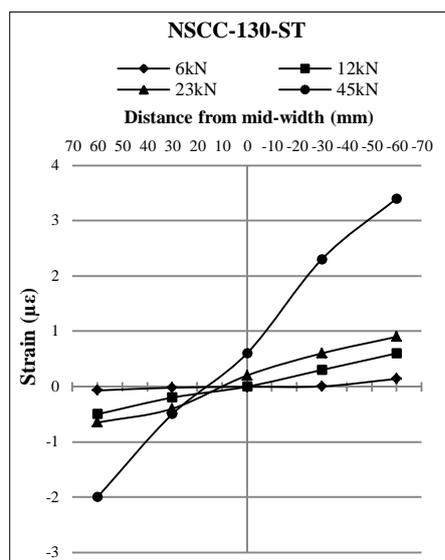
Figure 10. Concrete strain variation at the midpoint height of all tested columns with a load increasing

4. Conclusions

- Under an axial load, comparing by the normal strength concrete column reinforced with steel bars, a Geopolymer concrete column reinforced by GFRP bars gives some increase in the ultimate load (5.17%). But, under load eccentricity of 130 mm, a Geopolymer concrete column reinforced by GFRP bars gives a distinct increase in the ultimate load (69.37%). Thereupon, for the columns with high eccentricity, the geopolymer concrete column reinforced by GFRP bars increases the ultimate load capacity.

- For columns under pure compression, the concrete strain variations at midpoint height show wavy linear behavior or close to linear and become more uniform for columns having tension and compression zones.

- Under an axial load, based on the experimental results, the steel bars contributed about 16.47% at column capacity for NSCC-0-ST samples.

- Under an eccentric load, along with the height of the column, the calculated lateral deflection by the sine equation shows a high closeness to the experimental data. Such similarity was observed for all the samples at various loading stages until failure identified. With this regard, the above-mentioned equation can be utilized for the calculations of the geopolymer concrete columns reinforced by GFRP bars.

- The stiffness of the GPCC reinforced by the GFRP bars is more than that of NSCC reinforced by steel bars. This can be associated with the higher compressive strength of the GPCC than that of the NSCC.

- Under pure compression, failure of columns occurs suddenly due to cleavage of the concrete and simultaneously, rupturing of some longitudinal GFRP bars. With an increase in load eccentricity, the tension area appears and develops at the expense of a compression area. With this manner, due to spelling of the concrete cover, sudden failure changes to gradual one, (all these types of failure can be classified as compressive failure mode). With high eccentricity, gradual expanding the tension area expands gradually and the compression area reduces, even the remaining outermost concrete crumbles.

5. Conflicts of Interest

The authors declare no conflict of interest.

6. References

[1] Brown, M. C., "Corrosion Protection Service Life of Epoxy Coated Reinforcing Steel in Virginia Bridge Decks", PhD diss., Virginia Polytechnic Institute and State University, (2002).

[2] Benmokrane, Brahim, Ehab El-Salakawy, Amr El-Ragaby, and Thomas Lackey. "Designing and testing of concrete bridge decks reinforced with glass FRP bars." Journal of Bridge Engineering 11, no. 2 (2006): 217-229. doi: 10.1061/(asce)1084-0702(2006)11:2(217).

[3] Rizkalla, Sami, Tarek Hassan, and Nahla Hassan. "Design Recommendations for the Use of FRP for Reinforcement and Strengthening of Concrete Structures." Progress in Structural Engineering and Materials 5, no. 1 (January 2003): 16–28. doi:10.1002/pse.139.

[4] Juenger, Maria C.G., and Rafat Siddique. "Recent Advances in Understanding the Role of Supplementary Cementitious Materials in Concrete." Cement and Concrete Research 78 (December 2015): 71–80. doi:10.1016/j.cemconres.2015.03.018.

[5] Mehta, Kumar P. "Reducing the environmental impact of concrete." Concrete international 23, no. 10 (2001): 61-66.

[6] Kong, Daniel L.Y., and Jay G. Sanjayan. "Effect of Elevated Temperatures on Geopolymer Paste, Mortar and Concrete." Cement and Concrete Research 40, no. 2 (February 2010): 334–339. doi:10.1016/j.cemconres.2009.10.017.

[7] Davidovits, J., "High-alkali cements for 21st century concretes", Concrete technology past, present and future. ACI Special Publication, SP 144. Farmington Hills, Michigan, pp 383–398, (1994).

[8] Hardjito, Djwantoro, Steenie E. Wallah, Dody MJ Sumajouw, and B. Vijaya Rangan. "On the development of fly ash-based geopolymer concrete." Materials Journal 101, no. 6 (2004): 467-472.

[9] Duxson, Peter, John L. Provis, Grant C. Lukey, and Jannie S.J. van Deventer. "The Role of Inorganic Polymer Technology in the Development of 'green Concrete.'" Cement and Concrete Research 37, no. 12 (December 2007): 1590–1597. doi:10.1016/j.cemconres.2007.08.018.

[10] Mousavi, S. Hooman, M. R. Kavianpour, and O. Aminoroayaie Yamini. "Experimental Analysis of Breakwater Stability with Antifer Concrete Block." Marine Georesources & Geotechnology 35, no. 3 (May 24, 2016): 426–434. doi:10.1080/1064119x.2016.1190432.

[11] Hardjito, D, S E Wallah, D M J Sumajouw, and B V Rangan. "Fly Ash-Based Geopolymer Concrete." Australian Journal of Structural Engineering 6, no. 1 (January 2005): 77–86. doi:10.1080/13287982.2005.11464946.

[12] Rangan, B. V. "Studies on low-calcium fly ash-based geopolymer concrete." Indian Concrete Institute (2006): 9-17.

[13] Sofi, M., J.S.J. van Deventer, P.A. Mendis, and G.C. Lukey. "Engineering Properties of Inorganic Polymer Concretes (IPCs)." Cement and Concrete Research 37, no. 2 (February 2007): 251–257. doi:10.1016/j.cemconres.2006.10.008.

[14] Sarker, Prabir. "A constitutive model for fly ash-based geopolymer concrete." Archit Civil Eng Environ 1, no. 4 (2008): 113-20.

[15] Dattatreya, J. K., N. P. Rajamane, D. Sabitha, P. S. Ambily, and M. C. Nataraja. "Flexural behaviour of reinforced Geopolymer concrete beams." International journal of civil & structural engineering 2, no. 1 (2011): 138-159.

[16] Chang, E.H., "Shear and bond behaviour of reinforced fly ash-based geopolymer concrete beams", PhD diss., Curtin University of Technology; (2009).

[17] Razaqpur, A. Ghani, and Saverio Spadea. "Shear Strength of FRP Reinforced Concrete Members with Stirrups." Journal of Composites for Construction 19, no. 1 (February 2015): 04014025. doi:10.1061/(asce)cc.1943-5614.0000483.

[18] Oller, Eva, Antonio Marí, Jesús Miguel Bairán, and Antoni Cladera. "Shear Design of Reinforced Concrete Beams with FRP Longitudinal and Transverse Reinforcement." Composites Part B: Engineering 74 (June 2015): 104–122. doi:10.1016/j.compositesb.2014.12.031.

[19] Shahnewaz, Md, Robert Machial, M. Shahria Alam, and Ahmad Rteil. "Optimized Shear Design Equation for Slender Concrete Beams Reinforced with FRP Bars and Stirrups Using Genetic Algorithm and Reliability Analysis." Engineering Structures 107 (January 2016): 151–165. doi:10.1016/j.engstruct.2015.10.049.

[20] Ambily, P. S., C. K. Madheswaran, N. Lakhsmanan, J. K. Dattatreya, and S. A. Sathik. "Experimental studies on Shear behaviour of reinforced Geopolymer concrete thin webbed T-beams with and without fibres." International Journal of Civil & Structural Engineering 3, no. 1 (2012): 128-140.

[21] Pantelides, Chris P., Michael E. Gibbons, and Lawrence D. Reaveley. "Axial Load Behavior of Concrete Columns Confined with GFRP Spirals." Journal of Composites for Construction 17, no. 3 (June 2013): 305–313. doi:10.1061/(asce)cc.1943-5614.0000357.

[22] De Luca, A., F. Matta, A. Nanni, "Behavior of Full-Scale Glass Fiber-Reinforced Polymer Reinforced Concrete Columns Under Axial Load." ACI Structural Journal 107, no. 05 (2010). doi:10.14359/51663912.

[23] ACI (American Concrete Institute). "Guide for the design and construction of structural concrete reinforced with FRP bars." ACI 440.1 R-06 (2006).

[24] Canadian Standard Association. "CSA-S806-02, Design and Construction of Building Components with Fibre-Reinforced Polymers." Toronto, ON, Canada (2002).

[25] Deitz, D. H., I. E. Harik, and H. Gesund. "Physical properties of glass fiber reinforced polymer rebars in compression." Journal of Composites for Construction 7, no. 4 (2003): 363-366. doi:10.1061/(ASCE)1090-0268(2003)7:4(363).

[26] Fib Bulletin 40, "FRP reinforcement in RC structures", Stuttgart: The International Federation for Structural Concrete; (2007).

[27] Alsayed, S. H., Y. A. Al-Salloum, T. H. Almusallam, and M. A. Amjad. "Concrete columns reinforced by glass fiber reinforced polymer rods." Special Publication 188 (1999): 103-112.

[28] Tobbi, H., A.S. Farghaly, B. Benmokrane, "Concrete Columns Reinforced Longitudinally and Transversally with Glass Fiber-Reinforced Polymer Bars." ACI Structural Journal 109, no. 4 (2012). doi:10.14359/51683874.

[29] Sarker, Prabir Kumar. "Analysis of Geopolymer Concrete Columns." Materials and Structures 42, no. 6 (August 6, 2008): 715–724. doi:10.1617/s11527-008-9415-5.

[30] Sreenath, S, S Balaji, and K Saravana Raja Mohan. "Behaviour of Axially and Eccentrically Loaded Short Columns Reinforced with GFRP Bars." IOP Conference Series: Earth and Environmental Science 80 (July 2017): 012030. doi:10.1088/1755-1315/80/1/012030.

[31] Sumajouw, D. M. J., D. Hardjito, S. E. Wallah, and B. V. Rangan. "Fly Ash-Based Geopolymer Concrete: Study of Slender Reinforced Columns." Journal of Materials Science 42, no. 9 (December 12, 2006): 3124–3130. doi:10.1007/s10853-006-0523-8.

[32] Elchalakani, Mohamed, Ali Karrech, Minhao Dong, M.S. Mohamed Ali, and Bo Yang. "Experiments and Finite Element Analysis of GFRP Reinforced Geopolymer Concrete Rectangular Columns Subjected to Concentric and Eccentric Axial Loading." Structures 14 (June 2018): 273–289. doi:10.1016/j.istruc.2018.04.001.

[33] Elchalakani, Mohamed, Minhao Dong, Ali Karrech, Gang Li, Mohamed Sadakkathulla Mohamed Ali, and Allan Manalo. "Behaviour and Design of Air-Cured GFRP-Reinforced Geopolymer Concrete Square Columns." Magazine of Concrete Research 71, no. 19 (October 2019): 1006–1024. doi:10.1680/jmacr.17.00534.

[34] ACI Committee 211.1-91, "Standard Practice for Selecting Proportions for Normal Heavyweight, and Mass Concrete (ACI 211.1 - 91) Reapproved 1997, " Manual of Concrete Practices, American Concrete Institute, pp.1-38, (1991).

[35] Liu, Huihong, Zhean Lu, and Ziqiang Peng. "Test Research on Prestressed Beam of Inorganic Polymer Concrete." Materials and Structures 48, no. 6 (March 15, 2014): 1919–1930. doi:10.1617/s11527-014-0283-x.

[36] Duxson, P., A. Fernández-Jiménez, J. L. Provis, G. C. Lukey, A. Palomo, and J. S. J. van Deventer. "Geopolymer Technology: The Current State of the Art." Journal of Materials Science 42, no. 9 (December 19, 2006): 2917–2933. doi:10.1007/s10853-006-0637-z.

[37] ASTM C 469-02, "Standard Test Method for Static Modulus of Elasticity and Poisson's Ratio of Concrete in Compression", Annual Book of ASTM Standards, American Society for Testing and Materials, (2002).

[38] ASTM C 39/C 39M-05, "Standard Test Method for Compressive Strength of Cylindrical Concrete Specimens", Annual Book of ASTM Standards, American Society for Testing and Materials, pp.1-7, (2005).

[39] ASTM 496-02, "Standard Specification for Steel Wire, Deformed, for Concrete Reinforcement", ASTM Committee A-1 on Steel, Stainless Steel, and related Alloys, West Conshohocken, PA 19428- 2959, United States, 5 pp, (2002).

[40] ASTM D7205/D7205M-06, "Standard test method for tensile properties of fiber reinforced   polymer matrix composite bars", Conshohocken, PA: American Society for Testing and Materials; (2011).

[41] De Luca, Antonio, Fabio Matta, and Antonio Nanni. "Behavior of full-scale glass fiber-reinforced polymer reinforced concrete columns under axial load." ACI structural journal 107, no. 5 (2010): 589.

[42] Deitz, D. H., I. E. Harik, and H. Gesund. "Physical properties of glass fiber reinforced polymer rebars in compression." Journal of Composites for Construction 7, no. 4 (2003): 363-366. doi:10.1061/(ASCE)1090-0268(2003)7:4(363).